Proceedings of the 10th Brazilian Congress of Thermal Sciences and Engineering – ENCIT 2004
Braz. Soc. of Mechanical Sciences and Engineering – ABCM, Rio de Janeiro, Brazil, Nov. 29 – Dec. 03, 2004

Paper CIT04-0271

NUMERICAL SOLUTION OF VISCOELASTIC FREE SURFACE FLOWS USING THE PTT CONSTITUTIVE EQUATION

Gilcilene Sanchez de Paulo
gilcilene@lcad.icmc.usp.br

Murilo Francisco Tomé
murilo@lcad.icmc.usp.br

Fernando Marques Federson
fernando@lcad.icmc.usp.br

Antonio Castelo Filho
castelo@lcad.icmc.usp.br

José Alberto Cuminato
jacumina@lcad.icmc.usp.br

Instituto de Ciências Matemáticas e de Computação, ICMC, USP, Av. do Trabalhador São Carlense, 400 - Centro, 13560-970, Cx. Postal: 668, São Carlos, SP

Abstract. *This work is concerned with the development of a numerical technique for solving free surface flows described by the PTT model. The governing equations for incompressible isothermal viscoelastic flows described by the PTT model together with appropriate boundary conditions are given. The free surface stress conditions are treated in details. A formulation for calculating the extra stress components on rigid boundaries, following Tomé et al., 2002, is presented. The numerical technique presented in this work uses the finite difference method on a staggered grid and employs the ideas of the MAC (Marker-and-Cell) method. Numerical results demonstrating that this numerical technique can solve viscoelastic flows governed by the PTT model are presented. Moreover, validation results are given.*

keywords: *free surface flows, Phan-Thien-Tanner model, finite difference, marker-and-cell, jet buckling.*

1. Introduction

The investigation of the behaviour of viscoelastic free surface fluids in transient flows is very important in studying the rheological properties of viscoelastic materials and their processing. The non-linear viscoelastic constitutive equation Phan-Thien-Tanner (PTT) model (Phan-Thien and Tanner, 1977; Xue et al., 1998; Oliveira and Pinho, 1999; Alves et al., 2001; and Pinho et al., 2003) has been considered the more realistic model for polymer melts and concentrated solutions in comparison with other models. Therefore, in this paper the PTT model is adopted to model two-dimensional viscoelastic flows in the presence of moving free surfaces. A numerical technique capable of simulating viscoelastic free surface flows using the PTT constitutive equation is developed. The approach employed is based upon the SMAC (Simplified-Marker-and-Cell) method (Amsden and Harlow, 1970). The method described herein is applied to a two-dimensional channel flow and jet buckling (Cruickshank, 1988; Cruickshank and Munson, 1981; Tomé et al., 2002). The channel flow is used to validate the numerical method presented in this paper and it is shown that viscoelasticity has a strong influence on the jet buckling phenomenon. Moreover, it is shown that for the same nondimensional parameters Re, We and Fr differents jet buckling are obtained by varying the polymer-contributed viscosity. This paper is organized as follows: the governing equations are presented in Section 2; Section 3 presents the boundary conditions. The essence of the method is given in Section 4 while in Section 5 the basic finite difference equations are presented. Section 6 provides validation results and in Section 7 the numerical simulations of jet buckling are discussed.

2. Basic Equations

The basic equations governing incompressible isothermal flows described by the PTT model are the mass conservation equation, the equation of motion and the constitutive equation for the PTT model which in tensor

notation are given by

$$\frac{\partial u_i}{\partial x_i} = 0 \,, \tag{1}$$

$$\rho\frac{\partial u_i}{\partial t} + \rho\frac{\partial u_k u_i}{\partial x_k} = -\frac{\partial p}{\partial x_i} + \frac{\partial \tau_{ik}}{\partial x_k} + \rho g_i \,, \tag{2}$$

$$f(\tau_{kk})\tau_{ij} + \lambda \overset{\triangledown}{\tau}_{ij} = 2\eta_P D_{ij} \,. \tag{3}$$

where t is the time, $u_i = (u, v)$ is the velocity vector, p is the pressure, ρ is the density, g_i is the gravitational field, τ_{ik} is the extra stress tensor, which is related with kinematic quantities by the constitutive equation (3), $D_{ij} = \frac{1}{2}\left(\frac{\partial u_i}{\partial x_j} + \frac{\partial u_j}{\partial x_i}\right)$ is the rate of deformation tensor, λ is the fluid relaxation time, η_P is the polymer-contributed viscosity, $\overset{\triangledown}{(\cdot)}$ represents the following convected derivative:

$$\overset{\triangledown}{\tau}_{ij} = \frac{\partial \tau_{ij}}{\partial t} + \frac{\partial (u_k \tau_{ij})}{\partial x_k} - (L_{ik} - \xi d_{ik})\,\tau_{kj} - (L_{jk} - \xi d_{jk})\,\tau_{ki} \,,$$

and

$$f(\tau_{kk}) = 1 + \frac{\lambda\varepsilon}{\eta_P}\tau_{kk} \,,$$

where $L_{ij} = \partial u_i / \partial x_j$ is the velocity gradient tensor; ξ, ε are the parameters describing the PTT model. The Simplified PTT (SPTT) model is obtained by setting $\xi = 0$ (Phan-Thien and Tanner, 1977).

To solve Eqs. (1)–(3), we employ the EVSS formulation - Elastic-Viscous Stress - Splitting (Rajagopalan et al., 1990)

$$\tau_{ij} = 2\eta_N D_{ij} + \Sigma_{ij} \,, \tag{4}$$

where η_N is the Newtonian-contribuition viscosity, Σ_{ij} is the extra stress tensor, which is the polymer-contribuition stress.

Introducing the retardation ratio defined as $\beta = \eta_P/\eta_0$ with $\eta_0 = \eta_N + \eta_P$ being the total viscosity, it is interesting to remark that the Oldroyd-B model and the UCM model are special cases of the PTT model, if $\xi = 0$, $\varepsilon = 0$ and $\lambda_2 = (1-\beta)\lambda$ we obtain the Oldroyd-B model; in addition, if $\beta = 1$ we obtain the UCM model (Bird et al., 1977). Thus, $\eta_P = \beta\eta_0$ and $\eta_N = (1-\beta)\eta_0$.

Substituting Eq. (4) into Eq. (2) and Eq. (3) we obtain:

$$\rho\frac{\partial u_i}{\partial t} + \rho\frac{\partial u_k u_i}{\partial x_k} = -\frac{\partial p}{\partial x_i} + (1-\beta)\eta_0\frac{\partial}{\partial x_k}\left(\frac{\partial u_i}{\partial x_k}\right) + \frac{\partial \Sigma_{ik}}{\partial x_k} + \rho g_i \,, \tag{5}$$

$$f(\Sigma_{kk})\Sigma_{ij} + \lambda \overset{\triangledown}{\Sigma}_{ij} = 2\eta_0\left[\beta - (1-\beta)f(\Sigma_{kk})\right] D_{ij} - 2\lambda(1-\beta)\eta_0 \overset{\triangledown}{D}_{ij} \,, \tag{6}$$

with $f(\Sigma_{kk}) = 1 + \dfrac{\lambda\varepsilon}{\beta\eta_0}\Sigma_{kk}$.

Therefore, we shall solve the Eq. (1), (5) and (6) for the dependent variables u_i, p and Σ_{ij}.

We consider two-dimensional cartesian coordinate system $x_k = (x, y)$ and let L and U denote reference values for length and velocity and introduce the nondimensionalization

$$u_k = U\bar{u}_k, \qquad x_k = L\bar{x}_k, \qquad t = \frac{L}{U}\bar{t}, \qquad p = \rho U^2 \bar{p}, \qquad \Sigma_{ik} = \rho U^2 \bar{\Sigma}_{ik}, \qquad g_k = g\bar{g}_k.$$

Then Eqs. (1), (5) and (6) produce the following nondimensional equations (the bars have been dropped for convenience)

$$\frac{\partial u}{\partial x} + \frac{\partial v}{\partial y} = 0 \,, \tag{7}$$

$$\frac{\partial u}{\partial t} = -\frac{\partial u^2}{\partial x} - \frac{\partial (vu)}{\partial y} - \frac{\partial p}{\partial x} + (1-\beta)\frac{1}{Re}\left(\frac{\partial^2 u}{\partial x^2} + \frac{\partial^2 u}{\partial y^2}\right) + \frac{\partial \Sigma^{xx}}{\partial x} + \frac{\partial \Sigma^{xy}}{\partial y} + \frac{1}{Fr^2}g_x \,, \tag{8}$$

$$\frac{\partial v}{\partial t} = -\frac{\partial (uv)}{\partial x} - \frac{\partial v^2}{\partial y} - \frac{\partial p}{\partial y} + (1-\beta)\frac{1}{Re}\left(\frac{\partial^2 v}{\partial x^2} + \frac{\partial^2 v}{\partial y^2}\right) + \frac{\partial \Sigma^{xy}}{\partial x} + \frac{\partial \Sigma^{yy}}{\partial y} + \frac{1}{Fr^2}g_y \,, \tag{9}$$

$$\frac{\partial \Sigma^{xy}}{\partial t} = -f(\Sigma_{kk})\frac{1}{We}\Sigma^{xy} - \frac{\partial (u\Sigma^{xy})}{\partial x} - \frac{\partial (v\Sigma^{xy})}{\partial y} - \left[\left(\frac{\xi}{2}-1\right)\frac{\partial v}{\partial x} + \frac{\xi}{2}\frac{\partial u}{\partial y}\right]\Sigma^{xx} - \left[\left(\frac{\xi}{2}-1\right)\frac{\partial u}{\partial y} + \frac{\xi}{2}\frac{\partial v}{\partial x}\right]\Sigma^{yy}$$
$$+ \left[\beta - (1-\beta) f(\Sigma_{kk})\right]\frac{2}{ReWe}D^{xy} - (1-\beta)\frac{2}{Re}\left[\frac{\partial}{\partial t}D^{xy} + \frac{\partial (uD^{xy})}{\partial x} + \frac{\partial (vD^{xy})}{\partial y}\right.$$
$$\left. + \left(\frac{\partial u}{\partial y} - \frac{\partial v}{\partial x}\right)\frac{\partial u}{\partial x}\right], \tag{10}$$

$$\frac{\partial \Sigma^{xx}}{\partial t} = -f(\Sigma_{kk})\frac{1}{We}\Sigma^{xx} - \frac{\partial (u\Sigma^{xx})}{\partial x} - \frac{\partial (v\Sigma^{xx})}{\partial y} - 2(\xi-1)\frac{\partial u}{\partial x}\Sigma^{xx} - \left[(\xi-2)\frac{\partial u}{\partial y} + \xi\frac{\partial v}{\partial x}\right]\Sigma^{xy}$$
$$+ 2\left[\beta - (1-\beta) f(\Sigma_{kk})\right]\frac{1}{ReWe}D^{xx} - 2(1-\beta)\frac{1}{Re}\left[\frac{\partial}{\partial t}D^{xx} + \frac{\partial (uD^{xx})}{\partial x} + \frac{\partial (vD^{xx})}{\partial y}\right.$$
$$\left. + 2(\xi-1)\left(\frac{\partial u}{\partial x}\right)^2 + \frac{\xi}{2}\left(\frac{\partial v}{\partial x}\right)^2 + \left(\frac{\xi}{2}-1\right)\left(\frac{\partial u}{\partial y}\right)^2 + (\xi-1)\frac{\partial v}{\partial x}\frac{\partial u}{\partial y}\right], \tag{11}$$

$$\frac{\partial \Sigma^{yy}}{\partial t} = -f(\Sigma_{kk})\frac{1}{We}\Sigma^{yy} - \frac{\partial (u\Sigma^{yy})}{\partial x} - \frac{\partial (v\Sigma^{yy})}{\partial y} - 2(\xi-1)\frac{\partial v}{\partial y}\Sigma^{yy} - \left[(\xi-2)\frac{\partial v}{\partial x} + \xi\frac{\partial u}{\partial y}\right]\Sigma^{xy}$$
$$+ 2\left[\beta - (1-\beta) f(\Sigma_{kk})\right]\frac{1}{ReWe}D^{yy} - 2(1-\beta)\frac{1}{Re}\left[\frac{\partial}{\partial t}D^{yy} + \frac{\partial (uD^{yy})}{\partial x} + \frac{\partial (vD^{yy})}{\partial y}\right.$$
$$\left. + 2(\xi-1)\left(\frac{\partial v}{\partial y}\right)^2 + \frac{\xi}{2}\left(\frac{\partial u}{\partial y}\right)^2 + \left(\frac{\xi}{2}-1\right)\left(\frac{\partial v}{\partial x}\right)^2 + (\xi-1)\frac{\partial v}{\partial x}\frac{\partial u}{\partial y}\right], \tag{12}$$

where $f(\Sigma_{kk}) = 1 + ReWe\dfrac{\varepsilon}{\beta}(\Sigma_{kk})$; $Re = \rho UL/\eta_0$, $We = \lambda U/L$ and $Fr = U/\sqrt{L|g|}$ denote the Reynolds number, the Weissenberg number and the Froude number, respectively.

3. Boundary Conditions

To solve Eqs. (7)-(12) we need to specify appropriate boundary conditions for u_k and Σ_{ik}. On rigid boundaries the velocity must obey the no-slip condition $u_k = 0$ while on inflows it is prescribed by $u_n = U$ and $u_m = 0$ and on outflows we should have $\dfrac{\partial u_n}{\partial n} = \dfrac{\partial u_m}{\partial n} = 0$, where the subscripts n and m denote normal and tangential directions to the inflow/outflow. When calculating the velocity field and the non-Newtonian extra stress tensor, the values of the non-Newtonian extra stress tensor on the boundaries of the domain are required. They are obtained by the ideas of Tomé et al., 2002. On inflows we assume that $\Sigma^{xx} = \Sigma^{xy} = \Sigma^{yy} = 0$, (Marchal and Crochet, 1987; Mompean and Deville, 1997) and on outflows we employ $\dfrac{\partial \Sigma^{xx}}{\partial n} = \dfrac{\partial \Sigma^{xy}}{\partial n} = \dfrac{\partial \Sigma^{yy}}{\partial n} = 0$. On rigid boundaries, the components of the extra stress tensor are calculated from (10) – (12) which we assume to hold with the initial condition $\Sigma_{ik} = 0$. Following Tomé et al., 2002, it can be shown that on rigid boundaries parallel to the x-axis, Σ^{xx}, Σ^{yy} and Σ^{xy} are given by

$$\Sigma^{xy}(x,y,t+\delta t) = \left\{1 - \left[\xi^2 + 2(\varepsilon-1)\xi - 2\varepsilon\right]\frac{\delta t^2}{4}\left(\frac{\partial u(x,y,t+\delta t)}{\partial y}\right)^2\right\}^{-1}\left\{e^{-\frac{1}{We}\delta t}\Sigma^{xy}(x,y,t) - \left[\beta + \left(\frac{\xi}{2}+\varepsilon\right)\frac{\delta t}{2}\left[e^{-\frac{1}{We}\delta t}(\Sigma^{xx}(x,y,t)\right.\right.\right.$$
$$+ (2-\xi)We\beta\left(e^{\frac{1}{We}\delta t}-1\right)\left(\frac{\partial u(x,y,t^*)}{\partial y}\right)^2 + (2-\xi)\frac{\delta t}{2}\frac{\partial u(x,y,t)}{\partial y}\Sigma^{xy}(x,y,t)\Big)\Big] + \left(\frac{\xi}{2}+\varepsilon-1\right)\frac{\delta t}{2}\left[e^{-\frac{1}{We}\delta t}(\Sigma^{yy}(x,y,t)\right.$$
$$\left.\left.\left. - \xi We\beta\left(e^{\frac{1}{We}\delta t}-1\right)\left(\frac{\partial u(x,y,t^*)}{\partial y}\right)^2 - \xi\frac{\delta t}{2}\frac{\partial u(x,y,t)}{\partial y}\Sigma^{xy}(x,y,t)\right)\right]\right]\frac{\partial u(x,y,t+\delta t)}{\partial y} + e^{-\frac{1}{We}\delta t}\left[\beta - \left(\frac{\xi}{2}+\varepsilon\right)\frac{\delta t}{2}\Sigma^{xx}(x,y,t)\right.$$
$$\left. - \left(\frac{\xi}{2}+\varepsilon-1\right)\frac{\delta t}{2}\Sigma^{yy}(x,y,t)\right]\frac{\partial u(x,y,t)}{\partial y} + \beta e^{-\frac{1}{We}\delta t}\left(e^{\frac{1}{We}\delta t}-1\right)\frac{\partial u(x,y,t^*)}{\partial y}\Big\}, \tag{13}$$

$$\Sigma^{xx}(x,y,t+\delta t) = e^{-\frac{1}{We}\delta t}\left[\Sigma^{xx}(x,y,t) + (2-\xi)We\beta\left(e^{\frac{1}{We}\delta t}-1\right)\left(\frac{\partial u(x,y,t^*)}{\partial y}\right)^2 + (2-\xi)\frac{\delta t}{2}\frac{\partial u(x,y,t)}{\partial y}\Sigma^{xy}(x,y,t)\right]$$
$$+ (2-\xi)\frac{\delta t}{2}\frac{\partial u(x,y,t+\delta t)}{\partial y}\Sigma^{xy}(x,y,t+\delta t), \tag{14}$$

$$\Sigma^{yy}(x,y,t+\delta t) = e^{-\frac{1}{We}\delta t}\left[\Sigma^{yy}(x,y,t) - \xi We\beta\left(e^{\frac{1}{We}\delta t}-1\right)\left(\frac{\partial u(x,y,t^*)}{\partial y}\right)^2 - \xi\frac{\delta t}{2}\frac{\partial u(x,y,t)}{\partial y}\Sigma^{xy}(x,y,t)\right]$$
$$-\xi\frac{\delta t}{2}\frac{\partial u(x,y,t+\delta t)}{\partial y}\Sigma^{xy}(x,y,t+\delta t)\,. \tag{15}$$

whith $t^* \in (t, t+\delta t)$.

If the rigid boundary is parallel to the y-axis the calculation of $\Sigma^{xx}, \Sigma^{xy}, \Sigma^{yy}$ on the rigid boundary is similar to the case above.

3.1. Free Surface Stress Conditions

We consider transient free surface flows of viscous fluid flowing into a passive atmosphere and neglect surface tension effects. In this case, the appropriate boundary conditions on the free surface can be written as (Tomé et al., 2002)

$$p = 2(1-\beta)\frac{1}{Re}\left[\left(\frac{\partial u}{\partial x}{n_x}^2 + \left(\frac{\partial u}{\partial y}+\frac{\partial v}{\partial x}\right)n_x n_y + \frac{\partial v}{\partial y}{n_y}^2\right)\right] + \Sigma^{xx}{n_x}^2 + 2\Sigma^{xy}n_x n_y + \Sigma^{yy}{n_y}^2\,, \tag{16}$$

$$(1-\beta)\frac{1}{Re}\left[2\left(\frac{\partial u}{\partial x}-\frac{\partial v}{\partial y}\right)n_x n_y + \left(\frac{\partial u}{\partial y}+\frac{\partial v}{\partial x}\right)(n_y^2 - n_x^2)\right] + (\Sigma^{xx}-\Sigma^{yy})n_x n_y + \Sigma^{xy}(n_y^2 - n_x^2) = 0\,, \tag{17}$$

where $n_k = (n_x,\ n_y)$ is the normal outward unit vector to the free surface.

4. Numerical Method

To solve Eqs. (7)-(12) we employ the procedure used by Tomé et al., 2002. We suppose that at time t_0 the velocity field $u_i(x_k, t_0)$ and the non-Newtonian tensor $\Sigma_{ik}(x_k, t_0)$ are known and the values of u_i and Σ_{ik} on the boundary are given. To compute the velocity field $u_i(x_k, t)$ and the non-Newtonian tensor $\Sigma_{ik}(x_k, t)$, where $t = t_0 + \delta t$, we proceed as follows:

Step 1: Calculate a tentative velocity field, $\tilde{u}_i(x_k, t)$, from

$$\frac{\partial \tilde{u}_i}{\partial t} + \frac{\partial u_k u_i}{\partial x_k} = -\frac{\partial \tilde{p}}{\partial x_i} + (1-\beta)\frac{1}{Re}\frac{\partial^2 u_i}{\partial x_k^2} + \frac{\partial \Sigma_{ik}}{\partial x_k} + \frac{1}{Fr^2}g_i\,, \tag{18}$$

with $\tilde{u}_i(x_k, t_0) = u_i(x_k, t_0)$ using the correct boundary conditions for $u_i(x_k, t_0)$. The pressure field $\tilde{p}(x_k, t_0)$ can be arbitrary with the restriction that $\tilde{p}(x_k, t_0)$ must satisfy the pressure condition on the free surface (see Eq. (16)).

Step 2: Solve the Poisson equation: $\dfrac{\partial}{\partial x_k}\left(\dfrac{\partial \psi}{\partial x_k}\right) = \dfrac{\partial \tilde{u}_k}{\partial x_k}$. The appropriate boundary conditions for this equation are: $\dfrac{\partial \psi}{\partial n} = 0$ on rigid boundary and inflows and $\psi = 0$ on the free surface and outflows.

Step 3: Compute the final velocity: $u_i(x_k, t) = \tilde{u}_i(x_k, t) - \dfrac{\partial \psi(x_k, t)}{\partial x_i}$.

Step 4: Compute the pressure: $p(x_k, t) = \tilde{p}(x_k, t_0) + \dfrac{\psi(x_k, t)}{\delta t}$.

Step 5: Update the components of the non-Newtonian extra stress tensor according to the Eq. (13) – (15) derived in Section 3.

Step 6: Compute the components of the extra-stress tensor using Eq. (10) – (12).

Step 7: Update the marker particles positions. The last step in the calculation is to move the marker particles to their new positions. This is performed by solving $\dfrac{dx}{dt} = u$, $\dfrac{dy}{dt} = v$ by Euler's method. The fluid surface is defined by a list containing these particles and the visualization of the free surface is obtained by connecting them by straight lines.

5. Finite Difference Approximation

The equations describing the numerical method presented in Section 4 will be solved by the finite difference method on a staggered grid (see Fig. (1) a)) with cell dimensions $\delta x \times \delta y$. The pressure and the components of the non-Newtonian extra stress are located at cell centres (i, j) while the velocity u and v are staggered by $(i + 1/2, j)$ and $(i, j + 1/2)$, respectively. A scheme for identifying the fluid region and the free surface is employed. To effect this the cells in the mesh can be of several types, namely: cells Full of fluid (F), Surface cells (S), Empty cells (E), Inflow cells (I), Outflow cells (O) and Boundary cells (B). The F-cell is required to

contain fluid and to have no E-cell face in contact with any of its faces while S-cells are defined to contain fluid and to have at least one face in contact with an E-cell face. I-cells define an inflow boundary and O-cells define an outflow boundary. B-cells define rigid boundaries where the no-slip condition is imposed. Figure (1) b)) displays the types of cells within the mesh.

The time derivative in the Eq. (18) is approximated by the explicit Euler method which is first order. The pressure gradient and the linear terms of the momentum equations are approximated by central differences. For the convective terms we employ a high order upwind method. In this work the VONOS method – Variable Order Non-Oscilatory Scheme (Ferreira et al., 2002; Varonos and Bergeles, 1998) is employed to approximate the convective terms. The terms involving the divergent of the non-Newtonian extra stress are approximated by central differences. Therefore, the $\tilde{u}$-momemtum equation in the Eq. (18) is approximated by

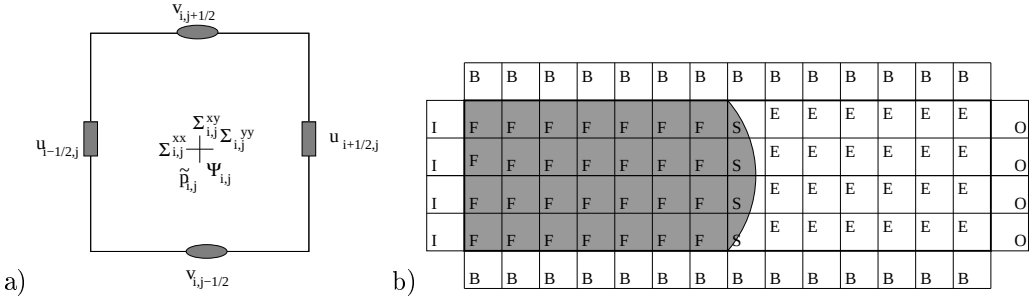

Figure 1: Types of cells in the domain.

$$\tilde{u}^{(n+1)}_{i+\frac{1}{2},j} = \tilde{u}_{i+\frac{1}{2},j} - \mathbf{conv}(u^2)_{i+\frac{1}{2},j} - \mathbf{conv}(vu)_{i+\frac{1}{2},j} - \frac{\tilde{p}_{i+1,j} - \tilde{p}_{i,j}}{\delta x} + (1-\beta)\frac{1}{Re}\left(\frac{u_{i+\frac{3}{2},j} - 2u_{i+\frac{1}{2},j} + u_{i-\frac{1}{2},j}}{\delta x^2} + \frac{u_{i+\frac{1}{2},j+1} - 2u_{i+\frac{1}{2},j} + u_{i+\frac{1}{2},j-1}}{\delta y^2}\right) + \frac{\Sigma^{xx}_{i+1,j} - \Sigma^{xx}_{i,j}}{\delta x} + \frac{\Sigma^{xy}_{i+\frac{1}{2},j+\frac{1}{2}} - \Sigma^{xy}_{i+\frac{1}{2},j-\frac{1}{2}}}{\delta y} + \frac{1}{Fr^2} g_x \,,$$

where terms like $\Sigma^{xy}_{i+\frac{1}{2},j+\frac{1}{2}}$ are obtained by averaging the four nearest values, e.g. $\Sigma^{xy}_{i+\frac{1}{2},j+\frac{1}{2}} := (\Sigma^{xy}_{i,j} + \Sigma^{xy}_{i+1,j} + \Sigma^{xy}_{i,j+1} + \Sigma^{xy}_{i+1,j+1})/4$. However, if the cell (i,j) is adjacent to a B-Cell or to an E-cell, a forward difference or a backward difference is used to approximate the derivatives $\frac{\partial \Sigma^{xy}}{\partial y}\Big|_{i+\frac{1}{2},j}$ and $\frac{\partial \Sigma^{xy}}{\partial x}\Big|_{i,j+\frac{1}{2}}$. The $\tilde{v}$-momemtum equation in Eq. (18) is approximated in the same manner. Thus, the approximations described for discretizing the momentum equations are second order in space and first order in time.

The Poisson equation (see Section 4 - Step 2) is discretized at cell centres using the five-point Laplacian, namely,

$$\frac{\psi_{i+1,j} - 2\psi_{i,j} + \psi_{i-1,j}}{\delta x^2} + \frac{\psi_{i,j+1} - 2\psi_{i,j} + \psi_{i,j-1}}{\delta y^2} = \frac{\tilde{u}_{i+\frac{1}{2},j} - \tilde{u}_{i-\frac{1}{2},j}}{\delta x} + \frac{\tilde{v}_{i,j+\frac{1}{2}} - \tilde{v}_{i,j-\frac{1}{2}}}{\delta y}. \tag{19}$$

Equation (19) leads to a symmetric and positive definite linear system for $\psi_{i,j}$. In order to solve this linear system we employ the conjugate gradient method. The final velocities are given by

$$u^{n+1}_{i+\frac{1}{2},j} = \tilde{u}_{i+\frac{1}{2},j} - \left(\frac{\psi_{i+1,j} - \psi_{i,j}}{\delta x}\right) \,, \qquad v^{n+1}_{i,j+\frac{1}{2}} = \tilde{v}_{i,j+\frac{1}{2}} - \left(\frac{\psi_{i,j+1} - \psi_{i,j}}{\delta y}\right)$$

and the pressure is calculated by

$$p_{i,j} = \widetilde{p}_{i,j} + \frac{\psi_{i,j}}{\delta t} \,.$$

The components of the non-Newtonian extra stress Eq. (10)– (12) are approximated by finite differences. The time derivative is explicitly approximated by the Euler method, the convective terms are computed using the VONOS method and the spatial first order derivatives are second order approximated. For instance, the component Σ^{xy} is computed as follows:

$$\Sigma^{xy(n+1)}_{ij} = -f(\Sigma_{kk})_{i,j}\frac{1}{We}\Sigma^{xy}_{ij} - \mathbf{conv}(u\Sigma^{xy})_{i,j} - \mathbf{conv}(v\Sigma^{xy}) - \left[\xi D^{xy}_{i,j} - \frac{v_{i+\frac{1}{2},j} - v_{i-\frac{1}{2},j}}{\delta x}\right]\Sigma^{xx} - \left[\xi D^{xy}_{i,j} - \frac{u_{i,j+\frac{1}{2}} - u_{i,j-\frac{1}{2}}}{\delta y}\right]\Sigma^{yy}$$
$$+[\beta - (1-\beta)f(\Sigma_{kk})_{i,j}]\frac{2}{ReWe}D^{xy}_{i,j} - (1-\beta)\frac{2}{Re}\left[\frac{1}{\delta t}\left(\left(D^{xy}_{i,j}\right)^{(n+1)} - \left(D^{xy}_{i,j}\right)\right) + \mathbf{conv}(uD^{xy})_{i,j} + \mathbf{conv}(vD^{xy})_{i,j}\right.$$
$$\left. + D^{xy}_{i,j}\frac{u_{i+\frac{1}{2},j} - u_{i-\frac{1}{2},j}}{\delta x}\right] \,, \tag{20}$$

where $D^{xy}_{i,j} = \frac{1}{2}\left(\frac{u_{i,j+\frac{1}{2}} - u_{i,j-\frac{1}{2}}}{\delta y} + \frac{v_{i+\frac{1}{2},j} - v_{i-\frac{1}{2},j}}{\delta x}\right)$ and $f(\Sigma_{kk})_{i,j} = 1 + \frac{\varepsilon}{\beta} ReWe(\Sigma^{xx}_{i,j} + \Sigma^{yy}_{i,j})$.

In Eq. (20), terms which are not defined at cell position are obtained by averaging, e.g.

$$u_{i,j+\frac{1}{2}} := \frac{u_{i+\frac{1}{2},j} + u_{i+\frac{1}{2},j+1} + u_{i-\frac{1}{2},j} + u_{i-\frac{1}{2},j+1}}{4}, \quad v_{i+\frac{1}{2},j} := \frac{v_{i,j+\frac{1}{2}} + v_{i+1,j+\frac{1}{2}} + v_{i,j-\frac{1}{2}} + v_{i+1,j-\frac{1}{2}}}{4}.$$

The free surface stress conditions eqs. (16) and (17) are approximated in the same way as in Tomé et al., 2002.

6. Validation of the Numerical Method

We validate the numerical technique presented in this paper by simulating the flow in a two-dimensional channel governed by the PTT Model. We consider a 2D-channel formed by two parallel walls at a distance L from each other and having a length of $10L$. At the channel entrance we impose the analitical profiles of fully developed flow given by

$$u(y) = -4y^2 + 4y\ , \qquad v = 0\ . \tag{21}$$

In this case, the constitutive equations Eqs.(10)–(12) reduce to

$$-f(\Sigma_{kk})\frac{1}{We}\Sigma^{xy} - \frac{\xi}{2}\frac{\partial u}{\partial y}\Sigma^{xx} - \left(\frac{\xi}{2}-1\right)\frac{\partial u}{\partial y}\Sigma^{yy} + [\beta - (1-\beta)f(\Sigma_{kk})]\frac{1}{ReWe}\frac{\partial u}{\partial y} = 0\,, \tag{22}$$

$$-f(\Sigma_{kk})\frac{1}{We}\Sigma^{xx} - (\xi-2)\frac{\partial u}{\partial y}\Sigma^{xy} - 2(1-\beta)\frac{1}{Re}\left(\frac{\xi}{2}-1\right)\left(\frac{\partial u}{\partial y}\right)^2 = 0\,, \tag{23}$$

$$-f(\Sigma_{kk})\frac{1}{We}\Sigma^{yy} - \xi\frac{\partial u}{\partial y}\Sigma^{xy} - (1-\beta)\xi\frac{1}{Re}\left(\frac{\partial u}{\partial y}\right)^2 = 0\,. \tag{24}$$

Equations (22)–(24) constitute a nonlinear system for Σ^{xy}, Σ^{xx} and Σ^{yy}. This nonlinear system has been solved by Newton's method employing Gaussian elimination with partial pivoting.

On the channel walls the no-slip condition is imposed and at the channel exit the conditions for outflow boundaries are applied (see Section 3). To simulate this problem the following input data was employed: $L = 1\ m$, $U = 1\ ms^{-1}$, $\nu = 2\ m^2s^{-1}$, $\lambda = 0.4\ s$, $\varepsilon = 0.001$, $\xi = 0.001$, $\beta = 0.2$, where ν is the kinematic viscosity defined by $\nu = \eta_0/\rho$. Hence $Re = LU/\nu = 0.5$ and $We = \lambda U/L = 0.4$. To demonstrate the convergence of the numerical method we ran this problem using three meshes as follows: M1 - (50×5 cells) $\delta x = \delta y = 0.2$; M2 - ($100 \times 10$ cells) $\delta x = \delta y = 0.1$ and M3 - (200×20 cells) $\delta x = \delta y = 0.05$. We started with the channel empty and injected fluid at the inflow until the channel became full and the steady state was reached. Under steady state conditions the velocity field and the viscoelastic extra-stress on the channel must have the same values as those imposed at the inflow (see Eqs. (21)–(24)). Figure (2) displays the values of the velocity field and the values of the non-Newtonian extra-stress components Σ^{xy}, Σ^{xx}, Σ^{yy} at the line $x = 5$ (middle of the channel) together with the respective analytic values (see Eq. (21) – (24)). The solid lines in Fig. (2) are the analytic solutions while the symbolds represent the numerical solutions obtained for the velocity field and the extra-stress components Σ_{ik} using the three meshes.

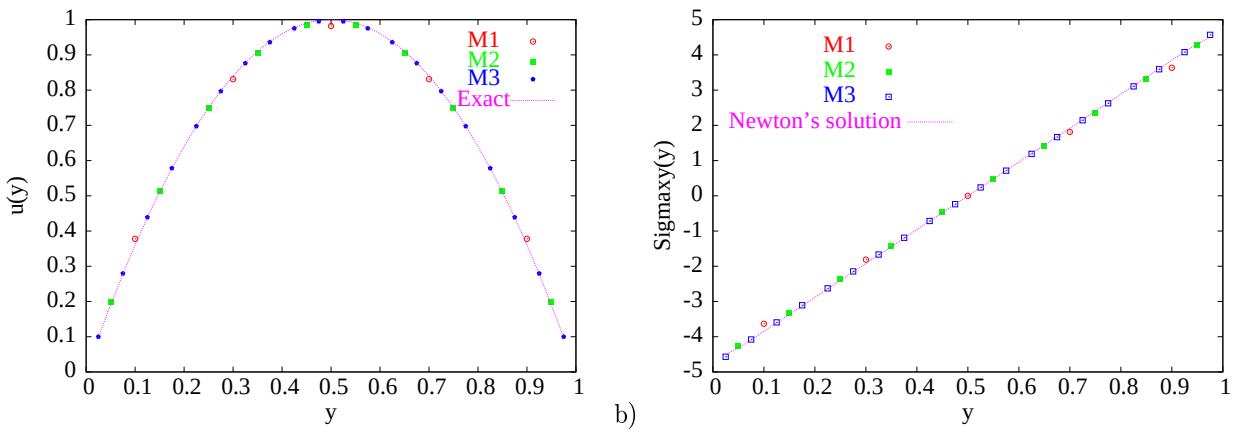

a) b)

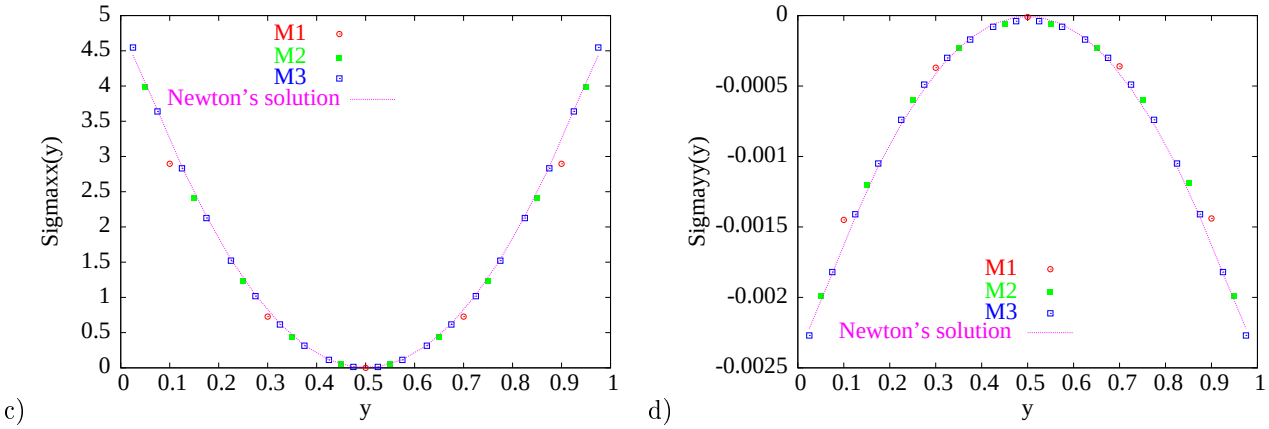

Figure 2: Numerical solution of 2D fully developed channel flow at $x = 5m$ and $t = 100s$: Comparison between numerical and analytic solutions. *a)* $u(y)$, *b)* $\Sigma^{xy}(y)$, *c)* $\Sigma^{xx}(y)$, *d)* $\Sigma^{yy}(y)$.

As we can see in Fig. (2) the agreement between the exact and the numerical solutions, which are represented by $(SolEx)$ and $(SolNum)$, respectively, is very good. Indeed, the relative l_2-norm of the errors,

$$E(SolNum) = \frac{\sum (SolEx - SolNum)^2}{\sum SolEx^2},$$

are displayed in Tab. (1) where we can see that the errors decrease with mesh refinement. These results demonstrate the convergence of the numerical method presented in this paper. These results were obtained using a dual Pentium III having a 1Ghz processor and 2Gb of ram memory. The CPU time spent on mesh M1 was approximately 10 minutes while for the intermediate mesh M2 the CPU time was about 150 minutes.

Table 1: Relative l_2-norm of the errors between the exact and the numerical solutions.

$Mesh$	$E(u)$	$E(\Sigma^{xx})$	$E(\Sigma^{xy})$	$E(\Sigma^{yy})$
$M1$	$4.23\,10^{-4}$	$11.09\,10^{-4}$	$7.45\,10^{-4}$	$13.90\,10^{-4}$
$M2$	$4.10\,10^{-5}$	$8.96\,10^{-4}$	$2.42\,10^{-4}$	$10.62\,10^{-4}$
$M3$	$5.00\,10^{-6}$	$2.77\,10^{-4}$	$6.00\,10^{-5}$	$5.38\,10^{-4}$

7. Numerical Simulation of jet buckling

To show that the technique presented in this paper can simulate viscoelastic free surface flows we applied it to simulate the buckling instability of thin jets. This problem has been investigated by several authors (Cruickshank, 1988; Cruickshank and Munson, 1981; Tomé et al., 2002) and a theory explaining this instability fully has not yet been presented. However, Cruickshank, 1988, has presented experimental and theoretical estimates predicting when a two-dimensional Newtonian jet will buckle. These estimates were based upon the jet width (L), the height of the inlet to the rigid plate (H) and the Reynolds number. From their study they concluded that if both conditions $Re < 0.56$ and $H/D > 3\pi$ are satisfied then a two-dimensional Newtonian jet will buckle. To illustrate that viscoelasticity has a strong influence on the jet buckling phenomenon we present three calculations: one calculation using a Newtonian fluid and two calculations employing the PTT Model. In these calculations we used the following input data: jet width $L = 6\ mm$, inlet velocity $U = 0.25\ ms^{-1}$, height of the inlet to the rigid plate $H = 5$cm, mesh spacing $\delta x = \delta y = 1\ mm$. The Newtonian fluid was defined by having a kinematic viscosity of $\nu_0 = 0.006\ m^2 s^{-1}$ and gravity was acting in the y-direction with $g_y = -9.81$. The PTT model was defined by having $\lambda = 0.036\ s$, $\eta_0 = 6\ Pa.s$ (since $\rho_0 = 1,000\ kgm^{-3}$), $\varepsilon = 0.01$, $\xi = 0.2$. In these calculations we used $\beta = 0.1$ and $\beta = 0.9$. The scaling parameters were L, U, λ, η_0, ρ_0 and g_y, giving $Re = UL/\nu_0 = 0.25$, $We = \lambda U/L = 1.5$ and $Fr = U/\sqrt{L|g|} = 1.030457$. In this case, the ratio $H/L = 8.3$ which does not satisfy Cruickshank's second condition and therefore the Newtonian jet should not buckle. The results of these calculations are displayed in Fig. (3). Indeed, Fig. (3) shows that the Newtonian jet does not undergo buckling confirming Cruickshank's prediction. However, the viscoelastic jets modelled by the PTT constitutive equation did undergo buckling. In the case of the PTT fluid when the bottom of the box, the viscosity which is given by the relation

$$\eta_p^1 = \frac{\tau^{yy} - \tau^{xx}}{D^{yy}}$$

is not constant within the jet. In fact, the viscosity of PTT fluid is varying during all the process while the Newtonian fluid has constant viscosity through the jet. Therefore Cruickshank's theory cannot be applied to the viscoelastic jet. Indeed, considering Fig. (3), at time $t = 0.14s$, the viscosity η_p^1 takes values which are larger than the Newtonian viscosity for both the cases of $\beta = 0.1$ and $\beta = 0.9$. These high viscosities make the fluid too viscous making the incoming fluid to accumulate and therefore leading to the buckling instability.

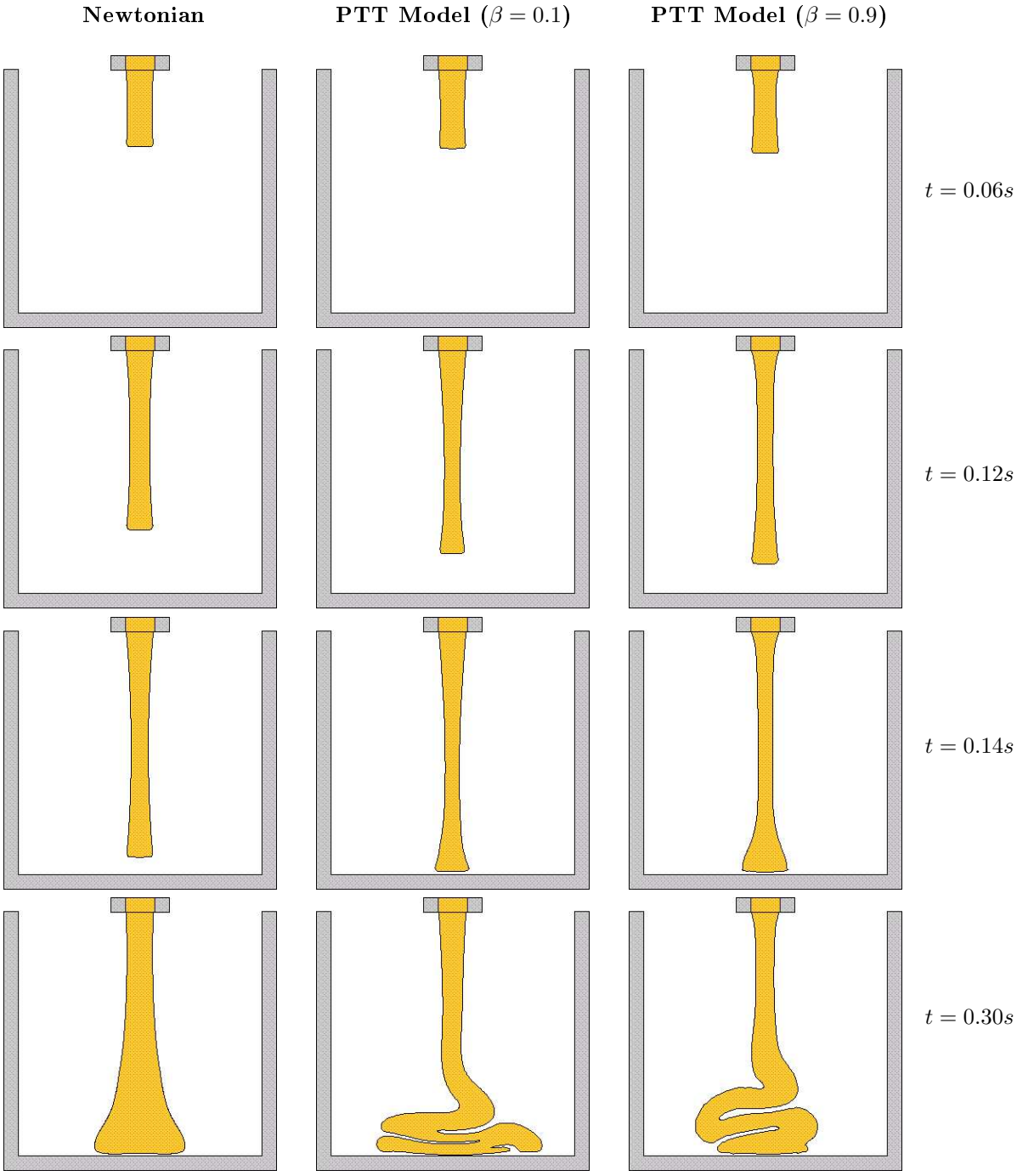

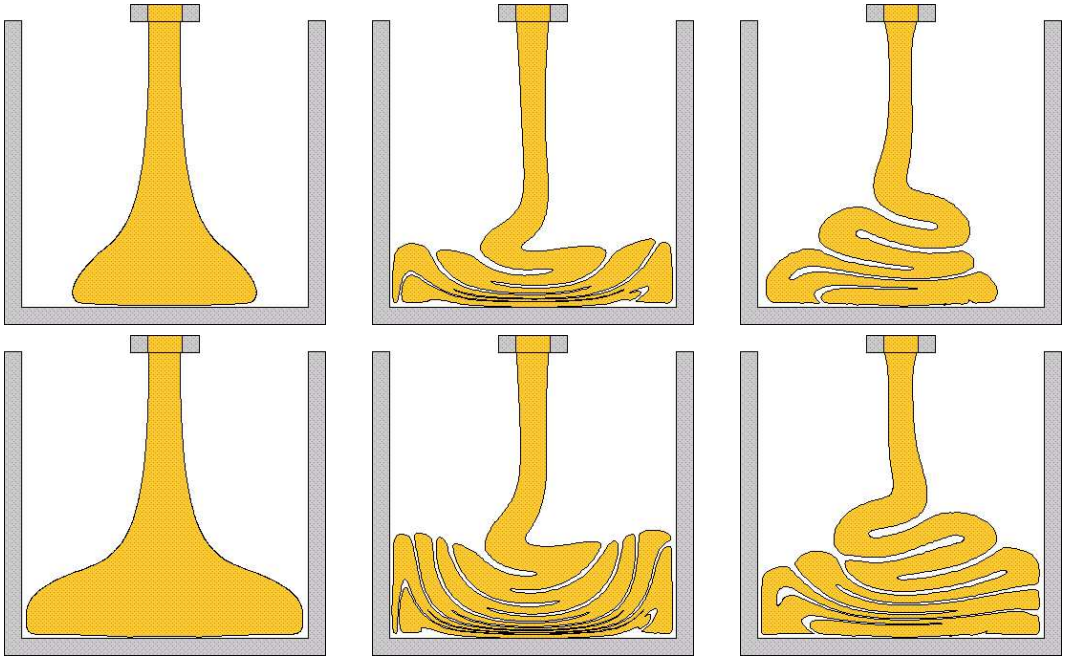

Figure 3: Numerical simulation of jet buckling: Fluid flow configuration at different times. $Re = 0.25$, $We = 1.5$, $\xi = 0.2$, $\varepsilon = 0.01$.

8. Concluding Remarks

This paper has been concerned with the development of a numerical method for solving the PTT model for free surface flows. The finite difference method described was validated by simulating the flow of a PTT fluid in a 2D channel. The numerical results were compared with analytic solutions and very good agreement was obtained. In addition, mesh refinement was performed which showed the convergence of the numerical method. The problem of jet buckling was simulated and it was found that viscoelasticity has a strong effect on the jet buckling instability. Moreover, it was shown that changing the parameter β affects the rheological behaviour of the fluid.

9. Acknowledgements

The authors would like to acknowledge the financial support of FAPESP (Fundação de Amparo a pesquisa do Estado de São Paulo) grants $02/00181-0$ and $00/03385-0$. The second author has been supported by CNPq (Conselho Nacional de Desenvolvimento Científico e Tecnológico) under grants $474040/2003-8$ and $523141/94$.

10. References

Alves, M., Pinho, F., and Oliveira, P., 2001, Study of steady pipe and channel flows of a single-mode Phan-Thien–Tanner fluid, "Journal of Non-Newtonian Fluid Mechanics", Vol. 101, pp. 55–76.

Amsden, A. and Harlow, F., 1970, The SMAC Method: A Numerical Technique for Calculating Incompressible Fluid Flows, Technical report, Los Alamos Scientific Laboratory Report LA–4370, Los Alamos, NM.

Bird, R., Armstrong, R., and Hassager, O., 1977, "Dynamics of Polymetric Liquids", Vol. 1, Wiley, New York, Fluid Mechanics.

Cruickshank, J. O., 1988, Low-Reynolds-number Instabilities in Stagnating Jet Flows, "Journal of Fluid Mechanics", Vol. 193, pp. 111–127.

Cruickshank, J. O. and Munson, B. R., 1981, Viscous-Fluid buckling of plane axisymmetric jets, "Journal of Fluid Mechanics", Vol. 113, pp. 221–239.

Ferreira, V., Tomé, M. F., N. Mangiavacchi, A. C., Cuminato, J., Fortuna, A. O., and Mckee, S., 2002, High-order upwinding and the hydraulic jump, "International Journal for Numerical Methods in Fluids", Vol. 39, pp. 549–583.

Marchal, J. and Crochet, M., 1987, A new mixed finite element for calculating viscoelastic flow, "Journal of Non-Newtonian Fluid Mechanics", Vol. 26, pp. 77–114.

Mompean, G. and Deville, M., 1997, Unsteady finite volume of Oldroyd-B fluid through a three-dimensional planar contraction, "Journal of Non-Newtonian Fluid Mechanics", Vol. 72, pp. 253–279.

Oliveira, P. and Pinho, F., 1999, Analytical solution for fully developed channel and pipe flow of Phan-Thien–Tanner fluids, "Journal of Fluid Mechanics", Vol. 387, pp. 271–280.

Phan-Thien, N. and Tanner, R. I., 1977, A new constitutive equation derived from network theory, "Journal of Non-Newtonian Fluid Mechanics", Vol. 2, pp. 353–365.

Pinho, F., Alves, M., and Oliveira, P., 2003, Benchmark solutions for the flow of Oldroyd-B and PTT fluids in planar contractions, "Journal of Non-Newtonian Fluid Mechanics", Vol. 110, pp. 45–75.

Rajagopalan, D., Armstrong, R., and Brown, R., 1990, Finite element methods for calculation of steady viscoelastic flow using constitutive equations with a Newtonian viscosity, "Journal of Non-Newtonian Fluid Mechanics", Vol. 36, pp. 159–192.

Tomé, M., Mangiavacchi, N., Castelo, A., Cuminato, J., and McKee, S., 2002, A finite difference techique for simulating unsteady viscoelastic free surface flows, "Journal of Non-Newtonian Fluid Mechanics", Vol. 106, pp. 61–106.

Varonos, A. and Bergeles, G., 1998, Development and assessment of a variable-order non-oscillatory scheme for convection term discretization, "International Journal for Numerical Methods in Fluids", Vol. 26, pp. 1–16.

Xue, S. C., Phan-Thien, N., and Tanner, R. I., 1998, Three-dimensional numerical simulation of viscoelastic flows through planar contractions, "Journal of Non-Newtonian Fluid Mechanics", Vol. 74, pp. 195–245.